

ASSESSMENT OF MULTICHANNEL AIRBORNE RADAR MEASUREMENTS FOR ANALYSIS AND DESIGN OF SPACE-TIME PROCESSING ARCHITECTURES AND ALGORITHMS*

William L. Melvin, Michael C. Wicks, and Russell D. Brown
United States Air Force Rome Laboratory
26 Electronics Parkway
Rome, NY 13441-4514

ABSTRACT

System design studies and detailed radar simulations have identified the utility of space-time adaptive processing (STAP) to accomplish target detection in cases where the target Doppler is immersed in sidelobe clutter and jamming. A recent US Air Force investment in STAP has produced a database of multichannel airborne data, through Rome Laboratory's Multichannel Airborne Radar Measurement (MCARM) program, to further develop STAP architectures and algorithms suited to operational environments. An aspect of actual data not typically incorporated into simulation scenarios is the nonhomogeneous features of real-world clutter and interference scenarios. In this paper we investigate the impact of nonhomogeneous data on the performance of STAP. Furthermore, we propose a preliminary scheme to detect and excise nonhomogeneous secondary data in the sample covariance estimation, thereby dramatically improving STAP performance as shown through a specific example using monostatic MCARM data.

1.0 INTRODUCTION

Current wide-area surveillance (WAS) demands focus on improved detection of low radial velocity and low radar cross-section targets by existing WAS platforms. Theoretical studies and computer simulations have identified space-time adaptive processing (STAP) as a potentially suitable technique to meet WAS objectives. To support the development and validation of STAP, the USAF Rome Laboratory has collected data under the Multichannel Airborne Radar Measurement (MCARM) program in collaboration with Westinghouse Electric Corporation. A more detailed description of the MCARM database is available in (Fenner, 1996). In this paper we consider the practical problem of applying STAP to actual airborne data, taken via the MCARM sensor. Measurement data, particularly data representative of mission-like scenarios, can appear severely nonhomogeneous in range due to spatially-varying clutter and interference statistics, exacerbated by array errors, airframe effects, etc. The nonhomogeneous characteristics of actual data can degrade STAP performance most directly by corrupting the estimation of the sample covariance matrix integral to the computation of the adaptive weights used to cancel clutter and interference.

Fundamentally, STAP is a two-dimensional filtering technique employed to maximize signal-to-clutter-plus-noise ratio (SCNR) through the adaptive control of spatial and/or Doppler sidelobes. In the optimum case, the linear combination of the weighted elements of the spatial-temporal data vector, X_k , into the scalar output, Y_k , via

$$Y_k = s^H R_k^{-1} X_k = \bar{w}_k^H X_k \quad (1)$$

maximizes SCNR and the probability of detection for gaussian-distributed interference (Brennan, 1973). In (1), s is the spatial-temporal steering vector, R_k is the *known* clutter-plus-noise covariance matrix, and \bar{w}_k are the resulting filter weights for range bin, k . In practice, the clutter and interference statistics are never known a priori, requiring R_k be replaced by the sample covariance matrix, \hat{R}_k , commonly computed via the maximum-likelihood estimate as

* Presented at the IEEE 1996 National Radar Conference, Ann Arbor, Michigan, 13-16 May 1996.

$$\hat{R}_k = \frac{1}{K} \sum_{i=1}^K Q_i Q_i^H \quad (2)$$

The secondary data vectors, Q_i , are the spatial-temporal data vectors, X_i , from those range cells other than the k^{th} range being tested for a target. Implementing (2) in practice requires the selection of K independent and identically distributed (iid) secondary data vectors. Selecting at least $K \approx 2N$ iid vectors, where N is the product of spatial channels and temporal pulses, yields an average loss ratio of less than 3 dB between the adaptive and optimal implementations (Reed, 1974). The challenge in a fielded STAP-based system then becomes finding a sufficient quantity of iid secondary data vectors to support the computation of (2). The difficulties associated with adequate sample support and non-iid data have been previously recognized by (Wang, 1994), for instance.

In this paper it is shown that the nonhomogeneous characteristics of actual airborne data can severely degrade STAP performance through the corrupted estimate of \hat{R}_k . We then propose a simple scheme to detect and excise questionable secondary data vectors to improve the estimation of \hat{R}_k , resulting in dramatically improved detection performance in an example employing actual MCARM data.

2.0 THE EFFECTS OF NONHOMOGENEOUS SECONDARY DATA

A secondary data vector, Q_i , is nonhomogeneous with respect to the data vector, X_k , if Q_i statistically departs from X_k in the structure of its covariance matrix, thereby violating the iid assumption critical to statistical estimation of \hat{R}_k , the sample covariance matrix of X_k . Rather than quantify the preceding definition of "nonhomogeneous", it is shown by example that the nonhomogeneous aspects of actual MCARM data can seriously degrade STAP capability. Also, it is shown that application of a nonhomogeneity detector aids selection of secondary data to compute (2), improving STAP performance and yielding results far exceeding that of digital beamforming (DBF).

As an example, a single coherent processing interval (CPI) of medium pulse repetition frequency (MPRF) MCARM data is processed for targets both adaptively and with DBF over range bins 270 to 360 (12.5 range bins \approx 1 nmi). The lowest complexity STAP architecture, Factored Time-Space, is employed solely as a means of illustrating the effects of nonhomogeneous data and its impact on the chosen adaptive algorithm. The Factored Time-Space method is post-Doppler, adaptive beamforming, with adaptive weights applied to the output of each Doppler filter. The Doppler filtering employs 128 pulses with a Hanning window function (1 Doppler bin \approx 3.9 kts). The first implementation of this architecture, hereafter solely referred to as FTS, selects N consecutive range cells on each side of the cell under test (CUT), excluding 2 guard cells, as secondary data. This "windowing" about the CUT is sensible if one assumes the closest range cells share similar statistical properties to the CUT and hence are approximately iid. The second implementation of the Factored Time-Space method, referred to as FTS_NH, uses a nonhomogeneity detector to sort all secondary data used in FTS over the entire range interval and select the $2N$, possibly nonconsecutive, secondary data appearing most homogeneous to improve estimation of the underlying clutter-plus-noise covariance matrix. This second approach also excludes the current CUT and 2 guard cells on each side. All 22 channels of the MCARM sensor are used in a planar 11 over 11 array, providing up to 11 adaptive nulls in azimuth and 1 adaptive null in elevation. Thus, $2N = 44$ range cells are selected for both FTS and FTS_NH.

Figures 1 and 2 compare the detection performance of the FTS and FTS_NH approaches for Doppler bins 6 and 10. A synthetic target has been injected into range bin 290 at Doppler bin 10. Both Doppler bins are in regions with the most severe clutter. The figures show the modified sample matrix inversion (MSMI) test statistic versus range for the given Doppler. The MSMI test statistic is given as

$$N_{MSMI} = \frac{\left| s^H \hat{R}_k^{-1} \bar{X}_k \right|^2}{s^H \hat{R}_k^{-1} s} \quad (3)$$

\bar{X}_k is the output of the selected Doppler filter for range k and \hat{R}_k is its covariance matrix estimate. MSMI has an embedded constant false alarm rate (CFAR) characteristic, implied by a threshold independent of range, and is

equivalent to cell averaging CFAR for this fixed threshold (W. Chen, 1991). Figure 1 shows the FTS_NH implementation dramatically suppresses clutter to the extent that a potential target at range bin 285 is easily identified by a selected, fixed threshold, with a separation of nearly 10 dB from the highest clutter peak. On the other hand, there is no way to identify this potential target with the FTS method without nonhomogeneity detection. Likewise, Figure 2 shows the FTS_NH approach allows improved detection of the injected target at range bin 290, whereas FTS corrupted by nonhomogeneities fails in this regard. Finally, Figure 3 shows the output of DBF for both Doppler bins 6 and 10, excluding CFAR processing. It is apparent from Figure 3 that both the potential and injected targets will go undetected.

Therefore, the preceding results show the nonhomogeneous features of actual airborne data may severely degrade STAP performance, as shown through a specific example using MCARM data. Furthermore, the results indicate that identification and excision of nonhomogeneous data leads to improved covariance estimation and a corresponding improvement in STAP detection potential. In the next section we discuss an approach for nonhomogeneity detection leading to the adaptive training strategy used to produce the FTS_NH results in this current section.

3.0 NONHOMOGENEITY DETECTION

The objective of nonhomogeneity detection is to identify data vectors which depart statistically in covariance structure from a reference vector, ideally taken from the CUT, and remove these data vectors from consideration in the sample covariance estimation of (2). Nonhomogeneity detection in this paper employs the generalized inner product as the distinguishing test statistic. The generalized inner product serves an over-all measure of the variability among the components available to estimate \hat{R}_k (P. Chen, 1995). It is a simple scalar measure of the covariance structure of a given data vector, X_k , and is expressed as

$$\Xi_k = X_k^H R_k^{-1} X_k ; \quad \Xi_k \rightarrow \hat{\Xi}_k \text{ for } R_k \rightarrow \hat{R}_k \quad (4)$$

The preceding choice of the generalized inner product as a nonhomogeneity detector contrasts with the selection of a power-based measure, given as $\mu_k = X_k^H X_k$, which only describes first-order statistical behavior. Two data vectors may have very similar powers (inner products), and yet have dissimilar covariance matrices. Figure 4 shows a plot of the sample generalized inner product and inner product for Doppler bin 6, normalized by the mean and ranked in ascending order. It is observed from the figure that the well-behaved features of the generalized inner product, such as moderate dynamic range and an identifiable "homogeneous" region indicated by the flatter-sloped region, lends itself to use as a practical nonhomogeneity (or alternatively, homogeneity) detector.

While the ultimate goal of this research is to select secondary data most homogeneous to the CUT for covariance training purposes, this preliminary version of nonhomogeneity detection merely uses (4) to identify the $2N$ most homogeneous secondary data vectors over a range interval. The initial assumption, based on the selected MCARM data file, postulates that a better estimation of the underlying clutter-plus-noise covariance suited to a majority of the range bins in the selected range interval, can dramatically improve STAP performance. Based on this fairly broad assumption, the performance improvement demonstrated in section 2.0 is both outstanding and likely can be improved upon further. The procedure to implement FTS_NH, yielding the results of section 2.0, is summarized in pseudocode as follows:

for Doppler = 1:Nt, %in section 2.0, Nt = 128 -- choose 1 receive direction, eg., broadside
for k = (range_start - N):(range_stop + N), %neglecting guard cells

$$\hat{R}_k = \frac{1}{2N} \sum_{i=k-N+1}^{k+N-1} \bar{X}_i \bar{X}_i^H ; \quad \hat{\Xi}_k = \bar{X}_k^H \hat{R}_k^{-1} \bar{X}_k ; \quad [\bar{Y}, I] = \text{sort} \left(\frac{\hat{\Xi}}{\text{mean}(\hat{\Xi})} \right) ;$$

- Select range index, I_r , corresponding to \bar{Y}_{I_r} satisfying $p_1 \leq \bar{Y}_{I_r} \leq p_2$, where p_1 and p_2 define the "homogeneity window" for the normalized, sorted $\bar{\Xi}_k$ defined by \bar{Y}_{I_r} , roughly centered about 1.0
- Recompute \hat{R}_k using secondary data selected via the chosen range indices from the previous step

- Compute N_{MSMI} according to (4) for $k = (\text{range_start}):(\text{range_stop})$, the desired range interval end;

end;

Note that the preceding nonhomogeneity detection scheme described for FTS_NH is applicable to other STAP architectures and algorithms. For example, JDL_NH, corresponding to the Joint Domain Localized architecture, is easily constructed from the FTS_NH pseudocode example above, and alternative adaptive algorithms such as Kelly's GLR are easily substituted for the MSMI algorithm (Wang, 1994). Also, it is noted that the nonhomogeneity detection scheme becomes more computationally efficient in light of the matrix inversion lemma (Haykin, 1984), allowing for a recursive formulation of the sample covariance matrix inverse. Thus, additional homogeneous secondary data and detected nonhomogeneities may be efficiently added and subtracted to and from \hat{R}_k^{-1} .

4.0 CONCLUSION

In this paper we demonstrate that the nonhomogeneous features of actual multichannel airborne data may seriously degrade the performance of STAP through a specific example using MCARM data. Degradation in performance results from poor sample covariance matrix estimates as shown in section 2.0, where it is also shown that an enhanced training strategy improves STAP effectiveness immensely. A good covariance estimate requires a sufficient quantity of iid secondary data with respect to the range cell being tested for a target. Traditional training strategies select secondary data by symmetrically windowing about the CUT, assuming nearest ranges will appear most similar in a second-order statistical sense. In section 3.0 we discuss the training approach used herein to better estimate the covariance matrix, leading to the dramatically improved STAP results of section 2.0. The superior training strategy described in section 3.0 selects secondary data nonconsecutively over a range interval, using the generalized inner product as a scalar measure of the variability of available secondary data vectors. Thus, data vectors most homogeneous in covariance structure, as measured by the generalized inner product, are selected to improve the estimation of the underlying clutter-plus-noise sample covariance matrix over an entire range interval. Use of this (non)homogeneity detection scheme is shown to greatly improve STAP performance potential for actual airborne data from the MCARM program and is considered an essential step in transitioning STAP to operational systems. Future work will concentrate on expanding the (non)homogeneity test to estimate a covariance matrix best matched to each individual range cell under test and iterative computation of selected training data.

5.0 REFERENCES

- L.E. Brennan and I.S. Reed, "Theory of Adaptive Radar", *IEEE Trans. AES*, Vol. AES-9, No. 2, pp. 237-252, March 1973.
- P. Chen, "Partitioning Procedure in Radar Signal Processing Problems", Final Report for Summer Faculty Research Program, Air Force Office of Scientific Research, Rome Laboratory, Rome, NY, August 1995.
- W.S. Chen and I.S. Reed, "A New CFAR Detection Test for Radar", *Digital Signal Processing*, Vol. 1, Academic Press, pp. 198-214, 1991.
- D.K. Fenner and W.F. Hoover, "Test Results of a Space-Time Adaptive Processing System for Airborne Early Warning Radar", In *The Record of the IEEE 1996 National Radar Conference*, Ann Arbor, MI, 13-16 May 1996.
- S. Haykin, "Introduction to Adaptive Filters", Macmillan, New York, NY, p. 138, 1984.
- I.S. Reed, J.D. Mallett and L.E. Brennan, "Rapid Convergence Rate in Adaptive Arrays", *IEEE Trans. AES*, Vol. AES-10, No. 6, pp. 853-863, November 1974.
- H. Wang and L. Cai, "On Adaptive Spatial-Temporal Processing for Airborne Surveillance Radar Systems", *IEEE Trans. AES*, Vol. 30, No. 3, pp. 660-670, July 1994.

6.0 FIGURES

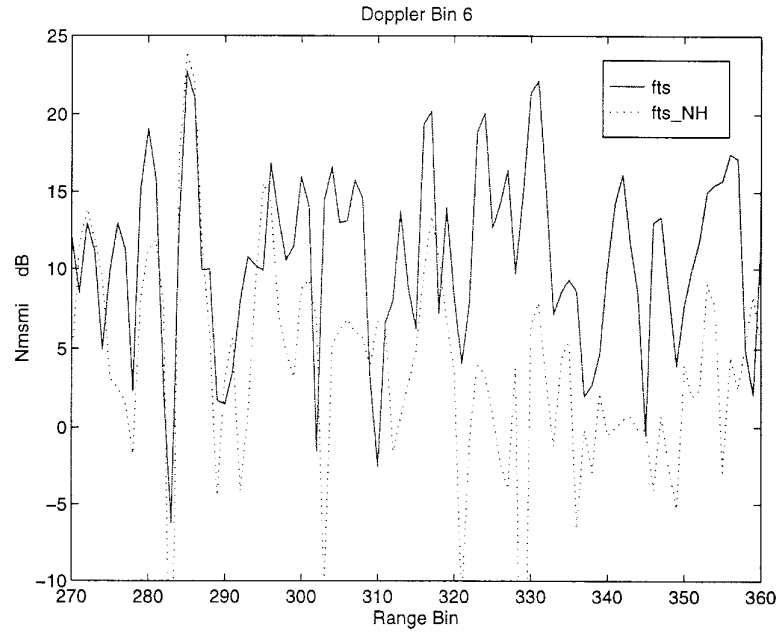


Figure 1. N_{MSMI} Vs. Range, Doppler Bin 6, MCARM Data.

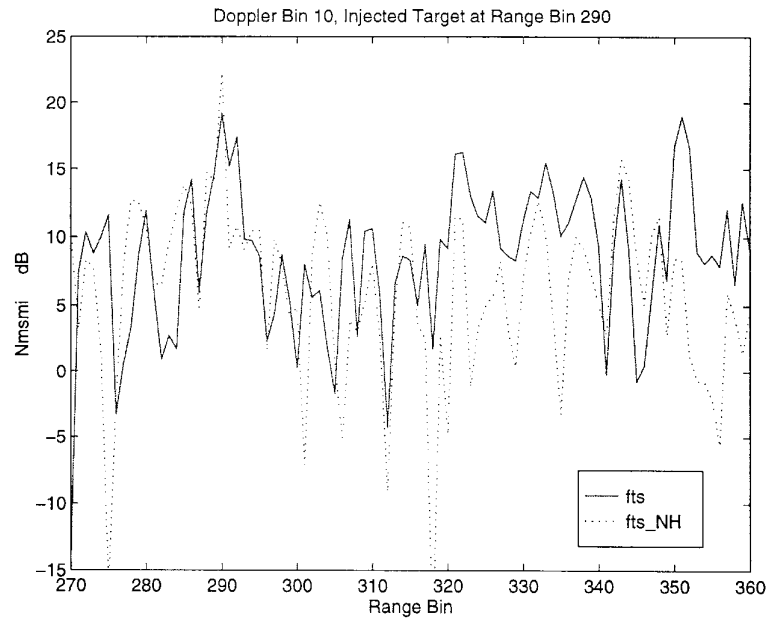


Figure 2. N_{MSMI} Vs. Range, Doppler Bin 10, Injected Target at Range Bin 290, MCARM Data.

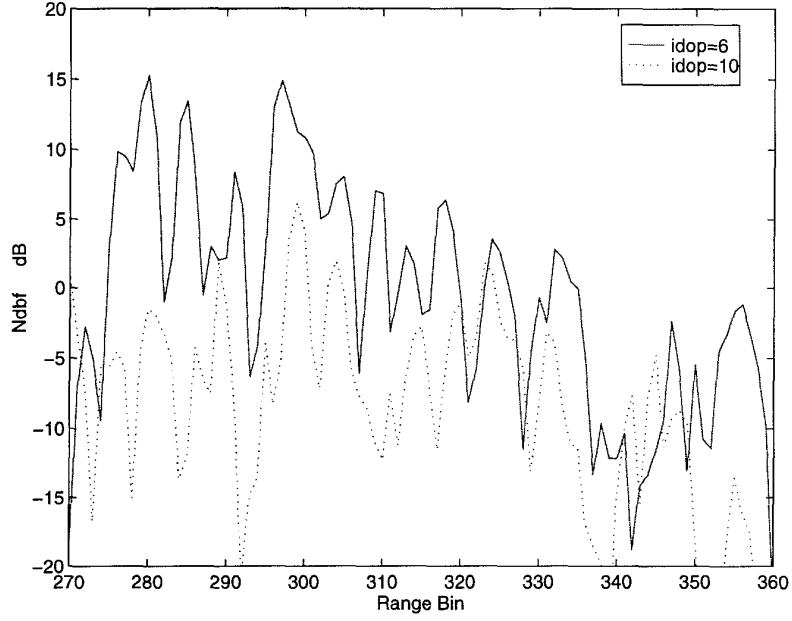


Figure 3. Digital Beamforming (DBF) Output Vs. Range, Doppler Bins 6 and 10, MCARM Data.

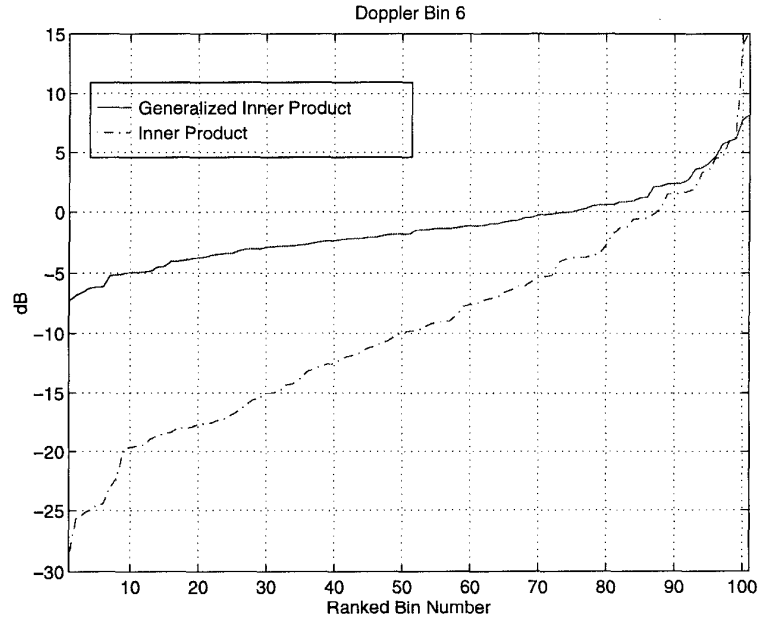


Figure 4. Normalized and Ranked Generalized Inner Product (4) and Inner Product, Doppler Bin 6, MCARM Data.

ACKNOWLEDGEMENT

The authors express their gratitude to Dr. Pinyuen Chen, Dr. Hong Wang, Dr. Yuhong Zhang, and Dr. Qingwen Zhang, all of Syracuse University, for their motivating input and discussion which has greatly benefitted this work.